communications materials

PERSPECTIVE

https://doi.org/10.1038/s43246-023-00336-9 OPEN

Piezoelectric response of disordered lead-based relaxor ferroelectrics

Tadej Rojac [1]✉

Lead-based relaxor ferroelectric perovskite oxides, exemplified by the (1-x)Pb($Mg_{1/3}Nb_{2/3}$)O_3-x$PbTiO_3$ (PMN-PT) solid solution, are a group of multifunctional materials with unique dielectric and piezoelectric properties. The long-lasting question that has intrigued the research community for decades is whether and to which extent the disordered relaxor nature of these materials is implicated in the exceedingly large piezoelectric response observed in both single crystals and ceramics. In this Perspective, focusing on PMN-PT, I briefly review and discuss the current understanding of the polar structure of relaxor ferroelectrics, followed by its possible implications in the large piezoelectricity. A critical review of the existing data confirms a significant progress made in recent years while opening up new questions related to the structure-property relations in these complex materials.

After more than seven decades of studies we are back in the era of relaxor ferroelectrics (FEs), a group of materials consisting of the unique combination of a disordered relaxor (RE) component and a long-range-ordered FE component. The group of RE-FEs includes a vast range of organic and inorganic materials, as well as lead-based and lead-free oxide compositions of various structural types[1–3]. The most discussed is the pseudo-binary (1–x)Pb($Mg_{1/3}Nb_{2/3}$)O_3–x$PbTiO_3$ (PMN–PT) solid solution where PMN and PT are the RE and FE end-members, respectively (note that throughout this paper PMN–PT will be in the focus and the terms "RE" and "RE-FE" will specifically refer to lead-based perovskite compositions). In contrast to "normal" FEs, canonical REs are distinguished by the temperature-dependent dielectric permittivity maximum that is typically broad and frequency dispersed (Fig. 1a). Among other useful properties of RE-FEs, the large permittivity over a broad temperature range is advantageous in diverse application areas, such as energy storage[4], electrocaloric cooling[5] and electrostrictive actuation[6].

A true interest in RE-FE single crystals began in 1997 when Park et al.[7] reported on the unusually large piezoelectric response (piezoelectric coefficient up to ~2500 pC/N) of PMN- and PZN-based rhombohedral crystals when measured along non-polar axis and in the vicinity of the morphotropic phase boundary (MPB; see red arrow in Fig. 1b). The large response was initially explained by first-principles computations using the concept of polarization rotation[8]. A simpler phenomenological approach later explained that the propensity for the polarization rotation has its origin in the structural instability related to the proximity of rhombohedral (R) and tetragonal (T) phases close to the MPB[9]. Therefore, by applying an electric field on the R crystal along its off-polar $[001]_{pc}$ direction, the field-driven rotation of the $[111]_{pc}$ R polarization vector toward the $[001]_{pc}$ T direction becomes easier in the proximity of the T phase (see inset of Fig. 1b), resulting in large piezoelectric coefficients measured in compositions close to the MPB (Fig. 1b, red arrow). Following the discoveries of the bridging monoclinic phases at MPBs in PZT and PMN–PT[10], the concept of polarization rotation has been universally used to explain MPB property enhancement[11]. As one of the points of discussion later in this contribution, it is important to emphasized that the polarization rotation in PMN–PT and similar RE-FEs is not as

[1] Electronic Ceramics Department, Jožef Stefan Institute, Jamova cesta 39, 1000 Ljubljana, Slovenia. ✉email: tadej.rojac@ijs.si

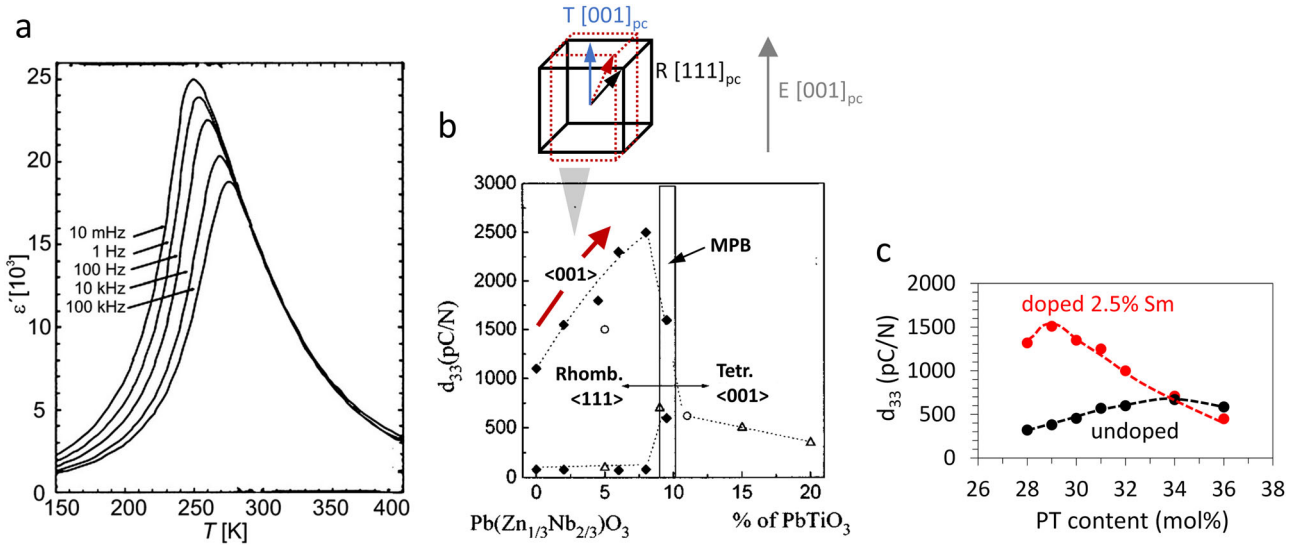

Fig. 1 Dielectric signatures and large piezoelectric response of lead-based RE-FE single crystals and ceramics. a Frequency dispersion of the temperature-dependent dielectric permittivity (ε′) maximum of PMN single crystal, representing the characteristic feature of RE-based materials[1,3]. **b** Piezoelectric d_{33} coefficient of RE-FE $Pb(Zn_{1/3}Nb_{2/3})O_3$–$PbTiO_3$ (PZN-PT) single crystals as a function of composition (PT content) and orientation (with respect to applied electric field), illustrating the large response of <001> -oriented rhombohedral (R) crystals close to the morphotropic phase boundary (MPB) region[7] (see red arrow). The source of the d_{33} data is reported in the original paper (Ref. [7]). The upper inset shows schematically the mechanism responsible for the large response, i.e., the easy rotation of the R $[111]_{pc}$ polarization vector (pc denotes pseudo cubic) toward the tetragonal (T) $[001]_{pc}$ polar direction in the case of the electric field (E) applied along $[001]_{pc}$ (see text for detailed explanation). **c** Piezoelectric d_{33} coefficient of PMN–PT ceramics as a function of PT content for undoped and Sm-doped ceramic samples, illustrating the ultrahigh piezoelectricity achieved by Sm doping. The data for undoped and Sm-doped PMN–PT were reproduced from Kelly et al.[54] and Li et al.[12], respectively. Figures shown in (**a**) and (**b**) were reprinted from Ref. [3] and Ref. [7] by permission from John Wiley & Sons and AIP Publishing, respectively.

simple as that in FE PZT because it is complicated by the disordered polar structure inherent to RE-based compositions (see next section for details).

PT-based RE-FE crystals has recently been overshadowed by the discovery of ultrahigh piezoelectricity in rare-earth doped PMN–PT ceramics[12]. With the strongest effect achieved using Sm doping, the authors reported on piezoelectric coefficients exceeding 1500 pC/N, which is more than doubled with respect to the response of the morphotropic undoped PMN–PT ceramics (see the maximum d_{33} values at the MPB in the two plots of Fig. 1c, i.e., 1500 pC/N for Sm-doped versus 650 pC/N for undoped PMN–PT ceramics). The piezoelectric enhancement was attributed to the local structural disorder introduced by the donor dopant[13], adding up to the already present disorder inherent to RE materials[14]. The multiple origins of the large response of donor-doped PMN–PT are still under debate with open questions regarding charged point defects and domain-wall pinning mechanisms influenced by the dopant[15].

In addition to their usefulness, the highly performant lead-based RE-FEs are also rich from a fundamental perspective and perhaps the most difficult to understand, particularly when it comes to structure-property relations[1]. Several different models have been proposed to explain the characteristic frequency dispersion of the temperature-dependent permittivity maximum[16–20] (Fig. 1a) and the polar structure of PMN and similar REs[14,21–26]. The key feature of RE-based materials is the existence of polar states correlated over a local, nanometer scale, traditionally referred to as the polar nanoregions (PNRs). Strongly supported by diffuse scattering data (see subsequent section for details and references), the dynamic behavior of PNRs under applied fields, alongside their freezing at lower temperatures, has been correlated with the characteristic dielectric dispersion[17]. The key question that has bothered the community for a long time is how and to which extent is the RE nature of these materials, and thus the nanoscale polar nature, implicated in their ultrahigh piezoelectric properties? Allowed by the fast development of theoretical and experimental methodologies (some of them are mentioned in subsequent sections), great advances have recently been made in deciphering the complex polar structure of RE-FEs and its role in the functional response. In this contribution, I will briefly review these issues focusing on the PMN–PT model system. The analysis of the current results suggests that there are still a number of details to be figured out, especially in relation to the complex link between the multiscale structure and macroscopic functional response. Filling such gaps may possibly allow to transfer the knowledge from lead-based to environmentally friendlier lead-free RE-FE materials.

Polar structure of RE-FE PMN–PT

The traditional view of the polar structure of REs consisting of PNRs dates back to the original study by Burns and Scott[27]. In their pioneering work the presence of small regions of polarization (size of several unit cells) below the critical temperature (later to be called the Burns temperature) was inferred from macroscopic optical measurements on $(Pb_{1-x}La_x)(Zr_{1-y}Ti_y)O_3$ ceramics and PMN single crystals. With no intention of criticizing any work, it is important to mention that derivations of microscopic mechanisms purely from macroscopic behavior of complex materials should be done with caution because it is not impossible that different microscopic mechanisms may result in the same or similar macroscopic physical properties. Nevertheless, the accepted picture of PNRs embedded into a non-polar matrix[1], depicted in Fig. 2a, has been extensively used for modelling neutron and X-ray diffuse scattering data of different RE and RE-FE materials[23] and also extended to involve a polar (FE) matrix instead of the non-polar (paraelectric) matrix[14,22,28]. Additional information on the local and average structure of PMN and PMN–PT, as provided by Neutron and X-ray scattering

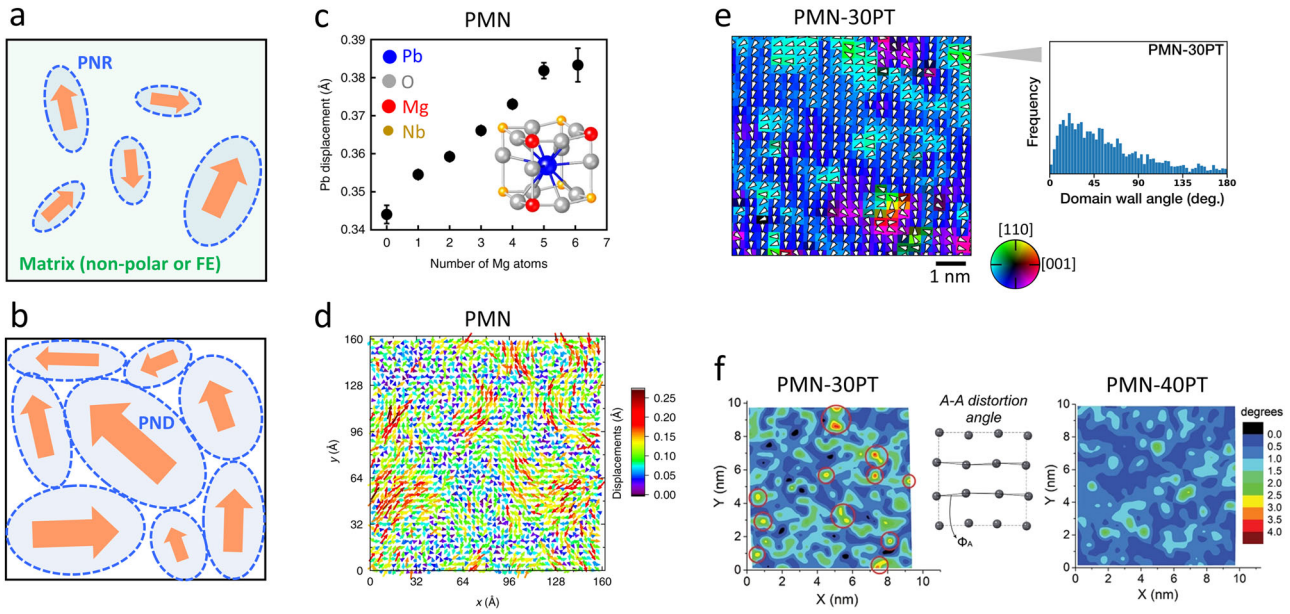

Fig. 2 Polar structure of PMN-PT. a Representations of two different microscopic polar states of RE-based materials consisting of (**a**) polar nanoregions (PNRs) embedded into a non-polar or ferroelectric (FE) matrix and (**b**) polar nanodomains (PNDs) separated by low-angle domain walls. The latter schematic was reproduced based on the study by Takenaka et al.[25] on PMN-PT and Eremenko et al.[26] on PMN; note that both these studies adopted combined theoretical and experimental approaches. **c** Correlation between Pb displacements from the center of the PbO_{12} cage (see inset) and number of surrounding B-site Mg ions in PMN; **d** projected Pb displacement map for PMN with arrows and colors indicating the direction and magnitude of the displacements, respectively. The data shown in (**c**, **d**) were extracted using reverse Monte Carlo simulations as reported by Eremenko et al.[26]. To be noted is that this method reported in Ref. [26] is based on PMN structural modelling by performing simultaneous refinements using a wide range of experimental dataset, including Neutron and X-ray powder total-scattering, extended X-ray absorption fine structure, 3D X-ray single-crystal diffuse-intensity distributions and Neutron Bragg profiles. **e** Projected polarization map of a region in PMN single crystal with 30 mol% PT (PMN–30PT) as determined from the difference of the center-of-mass positions of cations and anions using scanning transmission electron microscopy (STEM) analysis (see Kumar et al.[37]). The direction and magnitude of the off-centric displacements is indicated by the different colors and color brightness, respectively. The inset shows the extracted statistical distribution of domain-wall angles, confirming the presence of a large fraction of low-angle domain walls (peak at ~20°). **f** Maps of Pb distortion angle Φ_A (see inset) in PMN–30PT and PMN–40PT ceramics, illustrating the compositional dependence of the Pb positional disorder (original data are reported in Otonicar et al.[36]). Figures shown in (**e**) were reprinted from Ref. [37] by permission from Springer Nature.

experiments, can be found in the review article by Cowley et al.[29] (see also references therein).

The classical view of the polar state of REs (Fig. 2a) has been questioned by several authors[21,23,25] (it is encouraged to read the excellent comment-paper on this topic published by Hlinka[30]). In agreement with earlier diffuse scattering studies by Pasciak et al.[21], using molecular dynamics simulations on PMN–PT with 25 mol% PT (PMN-25PT), combined with experimental diffuse scattering data, Takenaka et al.[25] proposed an alternative scenario where the matrix of the PNRs is inexistent and the material is instead composed of densely packed polar nanodomains (PNDs) of several nanometers in size (~2–10 nm) separated by domain walls (Fig. 2b; note that the term PND is here used instead of PNR only to distinguish between the two different polar states shown in Fig. 2a and b). Based on the coexistence of multiple polar symmetries in PMN–25PT, it was reported that the change of polarization direction at the walls adopt, in average, low angles (~55°). The wide distribution of the domain-wall angles was proposed to arise due to the small energy differences between tetragonal-, orthorhombic- and rhombohedral-like orientations of local polarization. This is very different from the situation in normal FEs where polarization directions are restricted by the particular (single) polar symmetry, meaning that fewer domain walls and angles are possible (e.g., 180° and 90° walls in tetragonal FEs). The newly proposed polar structure of RE-FEs has opened interesting questions on how the so-called low-angle domain walls move and switch under applied external fields. To be noted, however, is that such dynamics was already discussed at least 25 years earlier within the model based on random fields in PMN[18] and in the frame of the PNR-breathing model[19].

The simplest crystal-chemical explanation for the disordered polar structure of lead-based REs considers the displacements of Pb cations, which crucially influence the local polarization[31]. To be recalled is that Pb displacements also play a fundamental role in the long-range polar ordering of conventional FEs, such as $PbTiO_3$[32]. Polar displacements of Pb cations in PMN are experimentally supported by various short-range-structure analyses, including nuclear magnetic resonance[33] and pair distribution function[34]. In lead-based perovskites the Pb cations are more sensitive to the B-site charge and strain disorder than the B-site cations themselves[31]. Figure 2c illustrates this point for PMN by revealing a nearly linear correlation between the Pb off-centric displacements from the center of PbO_{12} cage and the B-site chemistry represented here by the number of Mg cations in the surrounding B sites (see inset of Fig. 2c). The tendency of increased magnitude of Pb displacements with increasing Mg/Nb ratio is attributed to the Pb-O-Mg/Nb bonding interactions: the low ionic charge of Mg (2+) leads to underbonded oxygen, which is compensated by shorter Pb-O bonds and thus larger Pb displacements[26,31,35]. This chemically-driven disorder in the Pb displacements ultimately prevents the formation of a long-range FE order, leading to a disorder relaxor phase in which Pb displacements show quasi-ordered correlations extending on a short (nanoscale) range. Such correlations are evident in the Pb displacement map for PMN extracted using reverse Monte Carlo simulations (see reddish regions in Fig. 2d), which uses structural

refinements to different experimental diffraction and spectroscopic datasets. Interestingly, while this polar picture is overall compatible with the view of PNDs (Fig. 2b), the simulations revealed additional details of the hierarchical polar arrangements in PMN (details are out of scope of this Perspective paper and can be found in Ref. [26]). The chemical effect illustrated in Fig. 2c is also consistent with theoretical studies, confirming the essential role of the random electric fields (arising due to the random distribution of Mg^{2+} and Nb^{5+} cations on B sites) in the development of the nanoscale-correlated polar structure of PMN[24].

As the essential element of the PND scenario (Fig. 2b), the low-angle domain walls have been experimentally identified by atomic-scale scanning transmission electron microscopy (STEM) analysis in a wide range of PMN–PT compositions, first in ceramic samples[36], followed by single crystals (Fig. 2e; see also the inset showing the wide distribution of the domain-wall angles)[37]. It was found that these interfaces tend to be located at or close to the central regions of local structural heterogeneities, such as the chemical ordered regions and oxygen distortion and tilt regions[37]. This spatial correlation confirms that the heterogeneities play a role in disrupting the local polarization, affecting the domain structure and thus low-angle domain walls.

The positional disorder of Pb cations in PMN, led by the bonding interactions with the B-site cations (see Fig. 2c), is strongly affected by the incorporation of Ti cations on the B sites when forming the PMN–PT solid solution. Using atomic-resolution STEM imaging[36], a stronger disorder in the Pb-atom positions was consistently observed in PMN–PT ceramics with lower PT content (Fig. 2f). First-principles calculations revealed that the reduced Pb positional disorder by the addition of PT has to do with the effect of the Ti ions as they tend to stabilize collinear (ordered) Pb displacements of (100)-type[31]. The effect of Ti extends over multiple scales and shows up not only in the atomic structure (Fig. 2f), but also in the nano- and micro-scale domain structure, short- and long-range crystal symmetry and phase composition of PMN–PT as all these features develop with increasing PT content[36,38–41]. The implications of this multiscale structural evolution on the piezoelectric response of PMN–PT compositional series is presented in the next section.

Implications of the polar structure in the piezoelectric response of RE-FE PMN–PT

A great deal of studies has been performed to understand the implications of the RE nature on the large piezoelectric response of PMN–PT and similar RE-FEs. Different explanations have been proposed, including those based on polarization rotation with the bridging monoclinic phase (see first section and Refs therein), presence of nanoscale domains around MPB[38,42], critical points in the electric-field–temperature phase diagram[43], random electric fields[44], interaction between PNRs[45] or between PNRs and spontaneous polarization[14,46], and dynamics of low-angle domain walls[25,36]. All these complex mechanisms likely play a role and may dominate depending on the particular case. The most recent model by Li et al.[14], which was introduced using phase-field modeling, assumes the existence of PNRs inside a FE matrix (in accordance to Fig. 2a) where the PNR orientation changes with temperature. At cryogenic temperatures the polarization vectors of PNRs are presumably non-collinear with respect to the spontaneous FE polarization, P_s (Fig. 3a), whereby the collinear arrangement is achieved with increasing temperature. In this collinear state, under electric fields applied perpendicularly to the P_s direction, the PNRs can easily rotate helping the rotation of P_s in nearby regions (Fig. 3b). It is this mutual rotation mechanism that the authors used to explain why RE-FE PMN–PT single crystals have superior piezoelectric response than normal FEs, such as PZT.

To be noted is that the PNR-based mechanism presented in Fig. 3b is consistent with previous diffuse scattering studies, explaining the key role of the random electric fields on the high piezoelectricity of PMN–PT (as opposed to PZT in which such fields are absent)[44]. By invoking PNRs as characteristic polar features of REs, the model also provides a step forward in the understanding of the generalized polarization rotation mechanism as the origin of morphotropic property enhancements in PZT and PMN–PT[8–11]. In this aspect, the work by Manley et al.[46] has also to be emphasized. Based on a detailed neutron scattering analysis, the authors explain the dynamic role of PNRs in the elastic shear softening of the macroscopic polarization rotation in PMN–PT single crystals. In view of the criticism that this work received[47,48], it should be still mentioned that the general conclusion on the essential role of the nanoscale polar features in the piezoelectric response of PMN–PT is well supported by other studies[14,25,36,44,45], while the exact underlying mechanism(s) are still subject of debates.

Interestingly, the scenario proposed by Li et al. (Fig. 3a,b) assumes the existence of PNRs residing inside a long-range-ordered FE matrix (see Fig. 2a) and is thus in apparent contradiction with the picture of highly dense PNDs and low-angle domain walls where the matrix is nonexistent (see Fig. 2b). In addition, recent advances in diffuse scattering techniques[38] made it possible to identify a correlation between the increased properties at the MPB and the nanodomains, supporting the idea of the adaptive phase model[42]. It should be emphasized that, on the one hand, a number of microscopy[12,49] and diffuse scattering studies[22,28,50] report on the existence of different symmetries in PMN–PT and similar RE-FEs when the material is probed on different length scales, indirectly supporting the scenario depicted in Fig. 2a. However, on the other hand, it is equally important to mention the recent criticism to the diffuse scattering data on REs whose interpretation may be ambiguous considering that the data can be well represented by assuming either of the two polar states illustrated in Fig. 2a and b[21,30]. It is the personal opinion of the author of this paper that all these considerations leave open questions regarding the details of the mechanism(s) responsible for the large piezoelectricity of lead-based RE-FE ceramics and single crystals.

Most of the mechanisms used to describe the effect of the characteristic nanopolar structural features on the large piezoelectric response of PMN–PT are based on polarization rotation and thus lattice response to external fields. In view of the discovery of low-angle domain walls (see Fig. 2e), however, it is interesting to consider how these interfaces will respond to external fields and how their dynamics will be reflected in the macroscopic piezoelectricity across different parts of the PMN–PT phase diagram, not only close to the MPB.

Recent harmonic analysis of the nonlinear piezoelectric and dielectric properties of PMN–PT ceramics revealed a wide range of PMN-richer monoclinic compositions with the RE behavior exhibiting enhanced nonlinear response[36]. From the quasi-plateau of the irreversible Rayleigh coefficient, α^*, and the corresponding piezoelectric phase angle, $\tan\delta_p$, reached in the monoclinic M_B region (see the two red curves and red arrows in Fig. 3c), it was suggested that the enhanced irreversible (hysteretic) domain-wall contribution of these M_B compositions cannot be associated with the MPB effect. In fact, the MPB enhancements are clearly evident in the peaks of the reversible Rayleigh coefficient, d_{33}^{init}, occurring at the MPBs (see black curve in Fig. 3c). Additional third-harmonic polarization analysis made it possible to identify distinct regions in the phase diagram of PMN–PT, each showing a unique type of piezoelectric and

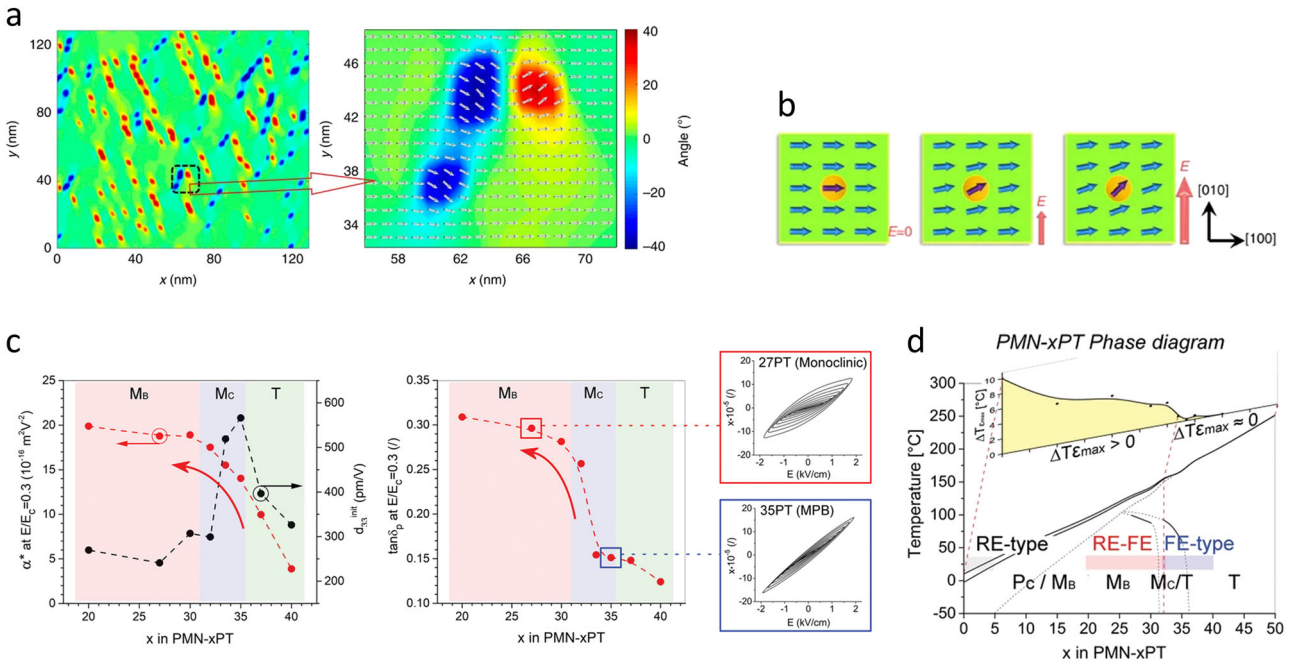

Fig. 3 Proposed mechanisms for the large piezoelectric response of PMN–PT single crystals and ceramics. a Phase-field simulated polar state at 100 K of a composite consisting of [100]-poled FE matrix (green) and inclusions of PNRs (red, yellow and blue). The x-and y-axes denote [100] and [010] direction, respectively, with the colors represent the direction of the local polarization. The right-hand inset shows an enlarged region highlighting the nano-sized PNRs with the different direction of polarization (different symmetry) with respect to that of the matrix FE phase. **b** Proposed mechanism of enhanced piezoelectric response of lead-based RE-FEs based on the polar state shown in (**a**). Green area and blue arrows represent the FE matrix and the associated polarization (P_s), respectively; yellow circles and purple arrows represent PNRs and their local polarization, respectively. The schematic shows the initial state at room temperature under no applied electric field E (left), where PNRs and P_s are nearly collinear, and under an applied E perpendicularly to the spontaneous polarization (P_s) of the FE matrix (middle and right schematic). The large piezoelectric response is explained by the rotation of PNRs along the E direction, which helps rotating the spontaneous polarization of the nearby FE region (details are reported in Ref. [14]). **c** Reversible (d_{33}^{init}) and irreversible (α^*) Rayleigh coefficients, and phase angle ($\tan\delta_P$) of PMN–PT ceramics as a function of PT content extracted from the field dependence of the converse piezoelectric response. The different colors mark the individual phase regions (M_B and M_C stand for monoclinic and T for tetragonal). The insets show piezoelectric hysteresis loops (displayed for increasing field amplitudes) representative of M_B (top) and MPB (bottom) composition. **d** Phase diagram of PMN–PT denoting the different types of nonlinear responses in the RE (gray), RE-FE (red) and FE (blue) regions of the PMN–PT system identified based on distinct third-harmonic responses (for details see Ref. [36]). The inset shows the frequency dispersion of the temperature-dependent maximum of the dielectric permittivity ($\Delta T_{\varepsilon max}$) as a function of PT content. The connecting line denotes the compositional point (~32 mol% PT) of the transition between the RE-FE-type and FE-type response coinciding with the drop of $\Delta T_{\varepsilon max}$ to zero.

dielectric nonlinear response (denoted in Fig. 3d as RE-, RE-FE- and FE-type). The pronounced hysteretic and nonlinear response of PMN-richer M_B composition showing RE behavior (see red-box inset of Fig. 3c) was contrasted with the more common Rayleigh-like response of PMN-poorer compositions where the RE behavior is not observed (see blue-box inset of Fig. 3c). The transition between these two types of responses at ~32 mol% PT was shown to occur at the point when the frequency dispersion of the temperature-dependent permittivity maximum drops to zero (see plot above the phase diagram in Fig. 3d and connecting line). Since this dispersion represents the fingerprint of the RE behavior, the enhanced nonlinear piezoelectricity of M_B compositions was attributed to the irreversible and reversible dynamics of low-angle domain walls. By quantifying the dynamic contribution of low-angle domain walls to the macroscopic piezoelectric response of PMN–PT ceramics, the results clearly point toward the extended effect of these RE-specific interfaces going well beyond MPB effects. While a similar nonlinear effect was also identified in lead-based compositions other than PMN–PT[36], it remains largely unexplored in lead-free RE-FE compositions.

Outlook

In this contribution, I reviewed and briefly discussed some of the current issues related to the polar structure of PMN-PT and similar lead-based RE-FEs alongside the implications of this structure in the large piezoelectric response of these materials. Despite intensive studies, it is found that the actual polar structure of lead-based RE-FEs is still an open issue with many details requiring further investigations. Considering that a clear microscopic picture of this structure is the precondition to understand the large macroscopic piezoelectric response of RE-FEs, it is not surprising that different, often incompatible explanations have been reported so far. A consensus on the unified microscopic description of the polar state in REs and RE-FEs has not been reached yet. However, the question is whether this is indeed necessary. As a matter of fact, it is not impossible that different polar states (such as those discussed in Fig. 2a, b) play a dominant role depending on the temperature, exact material composition (e.g., content of the RE phase, i.e., PMN, in PMN–PT) and material form (single crystal, ceramic or thin film), as, for example, indicated by some recent studies[51]. Complementary experimental and theoretical studies over wide material's length scale should be able to resolve this issue and provide guidance as to whether multiple models need to be elaborated.

The Pb-atom positional disorder triggered by the chemical bonding interactions with the multivalent B-site cations has been found to lie at the origin of the characteristic polar structure of PMN-PT. In the next step, it would be important to understand

how this disorder is affected by the application of an electric field, requiring state-of-the-art in situ STEM techniques. Although complicated and time consuming, in situ structural investigations on the atomic level should make it possible to visualize and comprehend the complex dynamics of the low-angle domain walls. In addition, an important advantage is that the problem of the local nature of the STEM analyses has been solved by statistical sampling[37]. The results of such in situ studies may have broader consequences considering that the low-angle-domain-wall dynamics was found to be responsible for the large nonlinear piezoelectric and dielectric response of a variety of lead-based RE-FEs with different B-site cations, including PMN–PT, $Pb(Sc_{0.5}Nb_{0.5})O_3$ and $Pb(Fe_{0.5}Nb_{0.5})O_3$[36].

An interesting point of discussion is whether the current knowledge of the mechanisms responsible for the large piezoelectric response of PMN–PT could be used to tailor functional properties of lead-free RE-FE materials. A system to possibly consider is the $BiFeO_3$–$BaTiO_3$ solid solution considering its robust, compositional-dependent RE-FE behavior[52] and the presence of Bi^{3+} cations with similar electronic structure as Pb^{2+} cations. While a rigorous local structural analysis of $BiFeO_3$–$BaTiO_3$ is still missing, it is interesting that the recently reported high piezoelectric activity of these ceramics achieved by a combination of Ga doping and quenching was found to be correlated with the increased lattice strain and tetragonality[53], reminiscent of the effect of Sm doping on the ultrahigh piezoelectricity of PMN-PT[12,13]. As a final note, it must be mentioned that systematic data on domain-wall contributions to the nonlinear dielectric and piezoelectric response of lead-free RE-FE ceramics, measured over wide compositional, temperature and driving-field ranges, are largely lacking. Such measurements would be useful to identify the piezoelectric contribution arising from the RE character of these materials, as recently demonstrated for PMN–PT[36].

Received: 16 June 2022; Accepted: 25 January 2023;
Published online: 15 February 2023

References

1. Bokov, A. A. & Ye, Z. G. Recent progress in relaxor ferroelectrics with perovskite structure. *J. Mater. Sci.* **41**, 31–52 (2006).
2. Chen, Q. et al. Relaxor ferroelectric polymers—fundamentals and applications. *Ferroelectrics* **354**, 178–191 (2007).
3. Shvartsman, V. V. & Lupascu, D. C. Lead-free relaxor ferroelectrics. *J. Am. Ceram. Soc.* **95**, 1–26 (2012).
4. Yang, L., Kong, X., Cheng, Z. & Zhang, S. Ultra-high energy storage performance with mitigated polarization saturation in lead-free relaxors. *J. Mater. Chem. A* **7**, 8573–8580 (2019).
5. Valant, M. Electrocaloric materials for future solid-state refrigeration technologies. *Prog. Mater. Sci.* **57**, 980–1009 (2012).
6. Nomura, S., Uchino, K. & Newnham, R. E. Large electrostrictive effects in relaxor ferroelectrics. *Ferroelectrics* **23**, 187–191 (1980).
7. Park, S. E. & Shrout, T. R. Ultrahigh strain and piezoelectric behavior in relaxor based ferroelectric single crystals. *J. Appl. Phys.* **82**, 1804–1811 (1997).
8. Fu, H. & Cohen, R. E. Polarization rotation mechanism for ultrahigh electromechanical response in single-crystal piezoelectrics. *Nature* **403**, 281–283 (2000).
9. Damjanovic, D. Comments on origins of enhanced piezoelectric properties in ferroelectrics. *IEEE Trans. Ultrason. Ferroelectr. Freq. Control* **56**, 1574–1585 (2009).
10. Noheda, B. Structure and high-piezoelectricity in lead oxide solid solutions. *Curr. Opin. Solid State Mater. Sci.* **6**, 27–34 (2002).
11. Damjanovic, D. Contributions to the piezoelectric effect in ferroelectric single crystals and ceramics. *J. Am. Ceram. Soc.* **88**, 2663–2676 (2005).
12. Li, F. et al. Ultrahigh piezoelectricity in ferroelectric ceramics by design. *Nat. Mater.* **17**, 349–354 (2018).
13. Li, F. et al. Giant piezoelectricity of Sm-doped Pb(Mg1/3Nb2/3)O3-PbTiO3 single crystal. *Science (80-.)* **364**, 264–268 (2019).
14. Li, F. et al. The origin of ultrahigh piezoelectricity in relaxor-ferroelectric solid solution crystals. *Nat. Commun.* **7**, 13807 (2016). The role of polar nanoregions in the large piezoelectric and dielectric response of classical lead-based relaxor ferroelectrics has been revelaed.
15. Li, Y., Borbely, M. & Bell, A. The influence of oxygen vacancies on piezoelectricity in samarium-doped $Pb(Mg_{1/3}Nb_{2/3})O_3$-$PbTiO_3$ ceramics. *J. Am. Ceram. Soc.* **104**, 2678–2688 (2021).
16. Cross, L. E. Relaxor Ferroelectrics. *Ferroelectrics* **76**, 241–267 (1987).
17. Viehland, D., Jang, S. J., Cross, L. E. & Wuttig, M. Freezing of the polarization fluctuations in lead magnesium niobate relaxors. *J. Appl. Phys.* **68**, 2916–2921 (1990).
18. Westphal, V., Kleemann, W. & Glinchuk, M. D. Diffuse phase transitions and random-field-induced domain states of the 'relaxor' ferroelectric $PbMg_{1/3}Nb_{2/3}O_3$. *Phys. Rev. Lett.* **68**, 847–850 (1992).
19. Glazounov, A. E. & Tagantsev, A. K. Crossover in a non-analytical behaviour of dielectric non-linearity in $PbMg_{1/3}Nb_{2/3}O_3$ relaxor ferroelectric. *J. Phys. Condens. Matter* **10**, 8863–8880 (1998).
20. Pirc, R. & Blinc, R. Spherical random-bond–random-field model of relaxor ferroelectrics. *Phys. Rev. B* **60**, 13470–13478 (1999).
21. Paściak, M., Wołcyrz, M. & Pietraszko, A. Interpretation of the diffuse scattering in Pb-based relaxor ferroelectrics in terms of three-dimensional nanodomains of the <110>-directed relative interdomain atomic shifts. *Phys. Rev. B* **76**, 014117 (2007).
22. Xu, G. Competing orders in PZN-xPT and PMN-xPT relaxor ferroelectrics. *J. Phys. Soc. Japan* **79**, 33–36 (2010).
23. Bosak, A., Chernyshov, D., Vakhrushev, S. & Krisch, M. Diffuse scattering in relaxor ferroelectrics: True three-dimensional mapping, experimental artefacts and modelling. *Acta Crystallogr. Sect. A* **68**, 117–123 (2012).
24. Al-Barakaty, A., Prosandeev, S., Wang, D., Dkhil, B. & Bellaiche, L. Finite-temperature properties of the relaxor $PbMg_{1/3}Nb_{2/3}O_3$ from atomistic simulations. *Phys. Rev. B* **91**, 214117 (2015).
25. Takenaka, H., Grinberg, I., Liu, S. & Rappe, A. M. Slush-like polar structures in single-crystal relaxors. *Nature* **546**, 391–395 (2017). A new polar-structure model based on low-angle domain walls has been proposed for lead-based relaxor ferroelectrics.
26. Eremenko, M. et al. Local atomic order and hierarchical polar nanoregions in a classical relaxor ferroelectric. *Nat. Commun.* **10**, 2728 (2019). Details of the structure and hierachical arrangments of polar nanoregions in canonical relaxor Pb(Mg1/3Nb2/3)O3 have been reported.
27. Burns, G. & Scott, B. A. Index of refraction in 'dirty' displacive ferroelectrics. *Solid State Commun.* **13**, 423–426 (1973).
28. Xu, G., Zhong, Z., Bing, Y., Ye, Z. G. & Shirane, G. Electric-field-induced redistribution of polar nano-regions in a relaxor ferroelectric. *Nat. Mater.* **5**, 134–140 (2006).
29. Cowley, R. A., Gvasaliya, S. N., Lushnikov, S. G., Roessli, B. & Rotaru, G. M. Relaxing with relaxors: a review of relaxor ferroelectrics. *Adv. Phys.* **60**, 229–327 (2011).
30. Hlinka, J. Do We Need the Ether of Polar Nanoregions? *J. Adv. Dielectr.* **2**, 1241006 (2012).
31. Grinberg, I. & Rappe, A. M. First principles calculations, crystal chemistry and properties of ferroelectric perovskites. *Phase Transitions* **80**, 351–368 (2007).
32. Cohen, R. E. Origin of ferroelectricity in perovskite oxides. *Nature* **358**, 136–138 (1992).
33. Blinc, R., Laguta, V. & Zalar, B. Field cooled and zero field cooled 207Pb NMR and the local structure of relaxor $PbMg_{1/3}Nb_{2/3}O_3$. *Phys. Rev. Lett.* **91**, 247601 (2003).
34. Jeong, I. K. et al. Direct observation of the formation of polar nanoregions in $Pb(Mg_{1/3}Nb_{2/3})O_3$ using neutron pair distribution function analysis. *Phys. Rev. Lett.* **94**, 147602 (2005).
35. Welberry, T. R., Goossens, D. J. & Gutmann, M. J. Chemical origin of nanoscale polar domains in $PbZn_{1/3}Nb_{2/3}O_3$. *Phys. Rev. B* **74**, 224108 (2006).
36. Otoničar, M. et al. Connecting the multiscale structure with macroscopic response of relaxor ferroelectrics. *Adv. Funct. Mater.* **30**, 2006823 (2020). The dynamic contribution of the low-angle domain walls to the nonlinear piezoelectric response of relaxor ferroelectric Pb(Mg1/3Nb2/3)O3–PbTiO3 was presented based on the nonlinear harmonic analysis.
37. Kumar, A. et al. Atomic-resolution electron microscopy of nanoscale local structure in lead-based relaxor ferroelectrics. *Nat. Mater.* **20**, 62–67 (2021). The link between the structural (and chemical) heterogeneities and the disordered polar structure in relaxor ferroelectric Pb(Mg1/3Nb2/3)O3–PbTiO3 has been discovered based on the atomic-scale microscopy analysis.
38. Krogstad, M. J. et al. The relation of local order to material properties in relaxor ferroelectrics. *Nat. Mater.* **17**, 718–724 (2018).
39. Matsuura, M. et al. Composition dependence of the diffuse scattering in the relaxor ferroelectric compound $(1-x)Pb(Mg_{1/3}Nb_{2/3})O_3$-$xPbTiO_3$ ($0 \le x \le 0.40$). *Phys. Rev. B* **74**, 144107 (2006).

40. Singh, A. K., Pandey, D. & Zaharko, O. Powder neutron diffraction study of phase transitions in and a phase diagram of (1-x)[$Pb(Mg_{1/3}Nb_{2/3})O_3$] -x$PbTiO_3$. *Phys. Rev. B* **74**, 024101 (2006).
41. Bai, F., Li, J. & Viehland, D. Domain hierarchy in annealed (001)-oriented $Pb(Mg_{1/3}Nb_{2/3})O_3$-x%$PbTiO_3$ single crystals. *Appl. Phys. Lett.* **85**, 2313–2315 (2004).
42. Jin, Y. M., Wang, Y. U., Khachaturyan, A. G., Li, J. F. & Viehland, D. Conformal miniaturization of domains with low domain-wall energy: Monoclinic ferroelectric states near the morphotropic phase boundaries. *Phys. Rev. Lett.* **91**, 1–4 (2003).
43. Kutnjak, Z., Petzelt, J. & Blinc, R. The giant electromechanical response in ferroelectric relaxors as a critical phenomenon. *Nature* **441**, 956–959 (2006).
44. Phelan, D. et al. Role of random electric fields in relaxors. *Proc. Natl. Acad. Sci. USA* **111**, 1754–1759 (2014).
45. Pirc, R., Blinc, R. & Vikhnin, V. S. Effect of polar nanoregions on giant electrostriction and piezoelectricity in relaxor ferroelectrics. *Phys. Rev. B* **69**, 212105 (2004).
46. Manley, E. M. et al. Giant electromechanical coupling of relaxor ferroelectrics controlled by polar nanoregion vibrations. *Sci. Adv.* **2**, e1501814 (2019).
47. Gehring, P. M. et al. Comment on "Giant electromechanical coupling of relaxor ferroelectrics controlled by polar nanoregion vibrations". *Sci. Adv.* **5**, 20–23 (2019).
48. Manley, E. M., Abernathy, L. D., Christianson, D. A. & Lynn, W. J. Response to comment on "Giant electromechanical coupling of relaxor ferroelectrics controlled by polar nanoregion vibrations". *Sci. Adv.* **5**, 3–5 (2019).
49. Kim, K. H., Payne, D. A. & Zuo, J. M. Symmetry of piezoelectric (1-x)$Pb(Mg_{1/3}Nb_{2/3})O_3$-x$PbTiO_3$ (x=0.31) single crystal at different length scales in the morphotropic phase boundary region. *Phys. Rev. B* **86**, 184113 (2012).
50. Wen, J., Xu, G., Stock, C. & Gehring, P. M. Response of polar nanoregions in 68% $Pb(Mg_{1/3}Nb_{2/3})O_3$ − 32% $PbTiO_3$ to a [001] electric field. *Appl. Phys. Lett.* **93**, 082901 (2008).
51. Fetzer, A. K., Wohninsland, A., Lalitha, K. V. & Kleebe, H. J. Nanoscale polar regions embedded within ferroelectric domains in Na1/2Bi1/2TiO3-BaTiO3. *Phys. Rev. Mater.* **6**, 1–10 (2022).
52. Zheng, T. & Wu, J. Perovskite $BiFeO_3$–$BaTiO_3$ ferroelectrics: Engineering properties by domain evolution and thermal depolarization modification. *Adv. Electron. Mater.* **6**, 2000079 (2020).
53. Lee, M. H. et al. Thermal quenching effects on the ferroelectric and piezoelectric properties of $BiFeO_3$-$BaTiO_3$ ceramics. *ACS Appl. Electron. Mater.* **1**, 1772–1780 (2019).
54. Kelly, J., Leonard, M., Tantigate, C. & Safari, A. Effect of composition on the electromechanical properties of (1-x)$Pb(Mg_{1/3}Nb_{1/3})O_3$-x$PbTiO_3$ ceramics. *J. Am. Ceram. Soc* **80**, 957–964 (1997).

Acknowledgements

The Slovenian Research Agency is acknowledged for the financial support (research core funding P2-0105 and research project J2-3042). I would personally like to thank Prof. Bokov for the critical comments to the manuscript and Editor Aldo Isidori for making the whole peer-review process a pleasant experience. I would not be able to write this Perspective without the numerous and priceless discussions with my coworkers at the department and beyond. This paper is dedicated to my father (*Dad, I'll keep going with the joyful thought of meeting you again*).

Author contributions

The author conceived the paper's idea, collected the data, prepared the figures and wrote the paper.

Competing interests

The author declares no competing interests.

Additional information

Correspondence and requests for materials should be addressed to Tadej Rojac.

Peer review information *Communications Materials* thanks Alexei Bokov and the other, anonymous, reviewer(s) for their contribution to the peer review of this work. Primary Handling Editor: Aldo Isidori.

Reprints and permission information is available at http://www.nature.com/reprints

Publisher's note Springer Nature remains neutral with regard to jurisdictional claims in published maps and institutional affiliations.